

Effect of Colloidal Catalysis on the Nanoparticle Size Distribution: Dendrimer–Pd vs PVP–Pd Nanoparticles Catalyzing the Suzuki Coupling Reaction[†]

Radha Narayanan and Mostafa A. El-Sayed*

Laser Dynamics Laboratory, School of Chemistry and Biochemistry, Georgia Institute of Technology, Atlanta, Georgia 30332-0400

Received: October 20, 2003; In Final Form: January 24, 2004

A comparison of the stability and catalytic activity of PAMAM–OH generation 4 dendrimer–Pd nanoparticles (1.3 ± 0.1 nm) with the previously studied PVP–Pd nanoparticles (2.1 ± 0.1 nm) in the Suzuki coupling reaction between phenylboronic acid and iodobenzene is conducted. After the first cycle, the average size of the PVP–Pd nanoparticles increases by 38% and the dendrimer–Pd nanoparticles increases by 54%. After the second cycle, the PVP–Pd nanoparticles decrease in size by 24% whereas the dendrimer–Pd nanoparticles continue to increase in size by 35%. The strong encapsulating action of the PAMAM–OH generation 4 dendrimer–Pd nanoparticles could make the rate of conversion to the full nanoparticle size slow, resulting in a large excess Pd metal atom concentration in solution, resulting in the continuous growth of the nanoparticles during the catalytic reaction. The effect of the individual reactants on the stability of the dendrimer–Pd nanoparticles has also been investigated and found to be similar to that observed for the PVP–Pd nanoparticles previously. It was found that the nanoparticle size growth occurs while refluxing in the presence of only the solvent, sodium acetate, or iodobenzene. However, the presence of phenylboronic acid is found to inhibit the particle growth, suggesting that it acts as a capping agent. Thus, the reaction mechanism must involve the adsorption of phenylboronic acid to the nanoparticle surface, which subsequently reacts with the iodobenzene in solution. This is similar to the mechanism found previously on PVP–Pd nanoparticles, suggesting that the mechanism is insensitive to the capping material used. The ratio of the yield of biphenyl formed in the second cycle to that in the first cycle is higher for the dendrimer–Pd nanoparticles catalyzed reaction than for the PVP–Pd nanoparticles. This could be due to the greater stability of the dendrimer–Pd nanoparticles and the increase in its size during the reaction. The larger PVP–Pd nanoparticles studied previously is believed to aggregate and precipitate out of solution during the second cycle. The presence of excess dendrimer is found to severely diminish the catalytic activity of the dendrimer–Pd nanoparticles and also diminishes the change in the Pd nanoparticle size during the catalysis.

Introduction

Due to their large surface-to-volume ratio, nanoparticles offer higher catalytic efficiency per gram than a larger size material. The field of nanocatalysis has been very active lately with numerous review articles published during the past decade in both heterogeneous catalysis in which the nanoparticles are supported on solid surfaces (e.g., silica or alumina)^{1–13} and in homogeneous catalysis with colloidal nanoparticles.^{14–21} Being small in size is expected to increase the nanoparticle surface tension. This makes surface atoms very active. Are they active enough to change the size and shape of the nanoparticles during catalysis? In the bulk of the catalysis with colloids, TEM characterization of the nanoparticles before and after catalysis is not given. However, there are a few studies in the literature where size distribution of the nanoparticles after recycling along with the catalytic activity is reported for characterization.^{22–28} There have also been some papers that discuss the catalytic activity of the nanoparticles upon recycling, but which do not examine the stability of the nanoparticles after catalysis.^{29–32} In a review of transition metal colloids as reusable catalysts,³³ it was pointed out that the major interest of the reusability of

nanoparticle catalysts has not been systematically studied or published in the metal colloid literature.

There have been very few detailed studies in the literature that examine the stability and catalytic activity of metal nanoparticles in colloidal solution that are used to catalyze various organic and inorganic reactions. In our previous study²² conducted with PVP–Pd nanoparticles catalyzing the Suzuki reaction between phenylboronic acid and iodobenzene, it was found that after the first cycle of the reaction, the nanoparticles increased in size, and this was attributed to the Ostwald ripening process. After the second cycle of the reaction, the nanoparticle size decreases and this was attributed to the larger nanoparticles aggregating and precipitating out of solution. It was also found that the Ostwald ripening process occurs in the presence of iodobenzene, whereas in the presence of phenylboronic acid, the process is greatly diminished. As a result, it was proposed that the mechanism involves phenylboronic acid binding to the nanoparticle surface and reacting with iodobenzene in solution.

The previous study with PVP–Pd nanoparticles raises some additional interesting questions. Does the method of preparing the nanoparticles used to catalyze the Suzuki reaction affect the particle growth process? Does the capping agent used affect the proposed mechanism of the Suzuki reaction? How does the

[†] Part of the special issue "Alvin L. Kwiram Festschrift".

* To whom correspondence should be addressed. E-mail: mostafa.el-sayed@chemistry.gatech.edu.

change in the size of the nanoparticles during the second cycle of the reaction affect the biphenyl product yield?

To shed light to these questions, the stability and catalytic activity of PAMAM–OH generation 4 dendrimer-capped Pd nanoparticles are examined and compared to those of the PVP–Pd nanoparticles studied previously. The use of dendrimer stabilized nanoparticles for catalyzing reactions has been a fairly recent activity. The first report of the use of dendrimers as capping agents in the preparation of metal nanoparticles is by the Crooks group.³⁴ A few examples of reactions catalyzed by dendrimer encapsulated nanoparticles include hydrogenation of olefins,^{35–37} Heck reactions,³⁸ oxidation reactions,³⁹ reduction reactions,⁴⁰ and Suzuki reactions.⁴¹ In a previous study,⁴¹ PAMAM–OH generation 2–4 dendrimers have been used as stabilizers for Pd nanoparticles in an effort to understand the effect of dendrimer generation on the catalytic activity of the nanoparticles catalyzing the Suzuki reaction. It was found that generation 2 dendrimers do not provide effective protective action whereas generation 3 and 4 dendrimers are good stabilizers. Palladium in PAMAM–OH generation 4 dendrimers is found to be the best catalyst because the dendrimer stabilizes the metal nanoparticles by preventing their agglomeration but it does not fully passivate the metal surface. A desirable property in a colloidal catalyst is to be small and stable, but with a nanoparticle surface that is not fully passivated so that reactants can access the encapsulated clusters.

The PAMAM–OH generation 4 dendrimer–Pd nanoparticles are prepared using the sodium borohydride reduction method whereas the PVP–Pd nanoparticles in the previous study²² were prepared using the ethanol reduction method. The aim of this paper is to study how the method of synthesizing the nanoparticles affects the particle growth process, how the capping agent affects the mechanism of the reaction, and how the size of the nanoparticles during the second cycle of the reaction affects the biphenyl product yield.

Experimental Section

Synthesis of PAMAM–OH Dendrimer Stabilized Pd Nanoparticles. The PAMAM–OH dendrimer stabilized Pd nanoparticles were synthesized in a manner similar to that described previously.⁴¹ The dendrimer solution was rotovaped to remove the methanol solvent. A 1 mM aqueous solution of the dendrimer and a 3 mM solution of K_2PdCl_4 were prepared. To prepare the nanoparticles, 90 mL of the dendrimer solution was added to 30 mL of the K_2PdCl_4 solution. The solution is stirred under nitrogen for 5 min. Then, 2 mL of 0.36 M of sodium borohydride was added to the solution. The solution was stirred vigorously under nitrogen atmosphere for 1 h. The 120 mL volume of nanoparticle solution was diluted to a total volume of 150 mL by adding 30 mL of doubly deionized water. The dilution was done so that the concentration of the initial Pd ions in the dendrimer-capped nanoparticles would be the same as for the PVP–Pd nanoparticles studied previously for comparison purposes. The diluted dendrimer–Pd nanoparticle solution was used for all of the experiments conducted. A JEOL 100C TEM is used to determine the average size and distribution of the nanoparticles.

Suzuki Reaction between Phenylboronic Acid and Iodobenzene. The Suzuki reaction between phenylboronic acid and iodobenzene was catalyzed using the PAMAM–OH generation 4 dendrimer-capped Pd nanoparticles as described previously.^{41–43} For this reaction, 0.49 g (6 mmol) of sodium acetate, 0.37 g (3 mmol) of phenylboronic acid, and 0.20 g (1 mmol) of iodobenzene was added to 150 mL of 3:1 acetonitrile:water solvent.

The solution was heated to 100 °C and 5 mL of the dendrimer-capped Pd nanoparticles was added to start the reaction. The reaction mixture was refluxed for a total of 12 h.

The same reaction mixture solution was used for recycling after the addition of fresh amounts of the reactants. For recycling, an assumption was made that all of the iodobenzene was used up because it is the limiting reactant. Initially, there was 1 mmol of iodobenzene and 3 mmol of phenylboronic acid present in the reaction mixture. After the first cycle, it was assumed that there is no iodobenzene left and that there was 2 mmol of phenylboronic acid left. As a result, for the second cycle, 1 mmol of iodobenzene and 1 mmol of phenylboronic acid were added. The reaction mixture was then refluxed for another 12 h to complete the second cycle.

TEM Studies. To examine the changes in the size distribution of the nanoparticles during the catalysis, samples of the reaction mixture before and after refluxing for 12 h were spotted onto Formvar stabilized copper TEM grids. The JEOL 100C TEM was used to determine the average widths and centers of the size distributions of the dendrimer–Pd nanoparticles after the first and second catalytic cycles. The effect of the amount of reduction time in synthesizing the nanoparticles was also examined. In addition, TEM was also used to examine the effect of the different chemicals present during the Suzuki reaction. The effects of refluxing for 12 h on the nanoparticle size distribution of the dendrimer–Pd nanoparticles in the presence of the solvent alone, in the solvent + sodium acetate, in the solvent + sodium acetate + phenylboronic acid, and in the solvent + sodium acetate + iodobenzene were investigated. The impact of adding excess dendrimer to the Pd nanoparticle solution before the reaction was also investigated.

For all of the above experiments, the concentration of the Pd ions present initially in the nanoparticles was 6.00×10^{-4} M and when 5 mL of the nanoparticles was added to 150 mL of the 3:1 acetonitrile:water solvent, the concentration of the Pd ions present initially was 1.94×10^{-5} M. For the experiments, the samples were spotted by placing a drop of the solution onto a Formvar stabilized copper grid and allowed to evaporate in air. The spotted samples took approximately 30 min to dry. Because the same deposition conditions were employed for all samples, the evaporation rate of the solvent was fairly reproducible from one sample to another. For each of the experiments, the internal reproducibility of the observed particle size and distribution was verified by spotting the sample onto 3 separate TEM grids. TEM images were also obtained from different sections of the TEM grids to verify the reproducibility of the particle size and distribution. The general reproducibility of the observed particle size and distribution was verified by conducting each experiment 3 times. As a result, it was possible to compare the particle size and distribution changes under various conditions.

The nanoparticle size and distribution were determined by counting approximately 1800 nanoparticles from 9 enlarged TEM images (approximately 200 nanoparticles from each TEM image). The size distribution plots were fit using a Gaussian model with Microcal Origin 5.0 graphing software to determine the widths and centers of the size distributions. The width of the distribution gives an idea of how narrow or wide the size distribution is and the center of the distribution is the most probable or average size of the nanoparticles (depending on the shape of the distribution).

HPLC Studies. The determination of the concentration of biphenyl product and thus the reaction yield were carried out by using the Hitachi-4500 HPLC equipped with a L4500A diode

TABLE 1: Summary of Widths and Centers of Size Distributions of PAMAM–OH Generation 4 Dendrimer Capped Pd Nanoparticles before and after Different Perturbations

| condition | before width (nm) | after width (nm) | before center (nm) | after center (nm) |
|---|-------------------|---|--------------------|---|
| Suzuki reaction | 0.7 ± 0.1 | after first cycle 2.2 ± 0.2 after second cycle 2.5 ± 0.1 | 1.3 ± 0.1 | after first cycle 2.0 ± 0.1 after second cycle 2.7 ± 0.1 |
| Suzuki reaction in the presence of dendrimer | 0.7 ± 0.1 | 1.3 ± 0.2 | 1.4 ± 0.1 | 1.7 ± 0.1 |
| reflux in solvent | 0.7 ± 0.1 | 1.6 ± 0.2 | 1.3 ± 0.1 | 2.5 ± 0.1 |
| reflux in solvent + dendrimer | 0.7 ± 0.1 | 1.5 ± 0.2 | 1.3 ± 0.1 | 1.7 ± 0.1 |
| reflux in solvent + sodium acetate | 0.8 ± 0.1 | 2.0 ± 0.2 | 1.3 ± 0.1 | 2.1 ± 0.3 |
| reflux in solvent + sodium acetate + phenylboronic acid | 0.7 ± 0.1 | 0.8 ± 0.1 | 1.3 ± 0.1 | 1.5 ± 0.1 |
| reflux in solvent + sodium acetate + iodobenzene | 0.7 ± 0.1 | 1.3 ± 0.2 | 1.3 ± 0.1 | 2.3 ± 0.2 |

TABLE 2: Comparison of the Percentage Change in the Centers and Widths of Distributions for the PVP–Pd Nanoparticles and the PAMAM–OH Generation 4 Dendrimer–Pd Nanoparticles as a Result of Catalyzing the Suzuki Reaction

| condition | % increase (+)/% decrease (–) in C_D and W_D of PVP–Pd nanoparticles (initially: 2.1 ± 0.1 nm) ²² | % increase (+)/% decrease (–) in C_D and W_D of PAMAM–OH generation 4 dendrimer–Pd nanoparticles (initially: 1.3 ± 0.1 nm) |
|---------------------------------|--|--|
| first cycle of Suzuki reaction | $C_D = +38 \pm 10\%$ $W_D = +155 \pm 18\%$ | $C_D = +54\%$ $W_D = +186\%$ |
| second cycle of Suzuki reaction | $C_D = -24 \pm 3\%$ $W_D = -68\%$ | $C_D = +35\%$ $W_D = +14\%$ |

array detector in which the absorbance at 254 nm was monitored. The separation was carried out on a reversed-phase packed column (Rainin Microsorb-MV C18, 300 Å, dimensions 4.6 × 250 mm) using a 60:40 acetonitrile–water mixture and a flow rate of 1 mL/min. The area of the chromatographic peaks was calculated with a D-6000 interface-integrator. A calibration curve for determining the concentration of biphenyl was constructed by plotting the peak area vs concentration of biphenyl standards. The standards prepared were 0.0005, 0.001, 0.0015, 0.002, 0.0025, and 0.003 M biphenyl. For HPLC measurements, all samples were diluted to one-fourth of the original concentration so that the peak areas will be within the range of the calibration curve. The concentration of biphenyl was determined before the first cycle, after the first cycle, before the second cycle, and after the second cycle. Also, the effect of the presence of excess dendrimer on the amount of biphenyl formed was determined.

Results and Discussion

Effect of Nanoparticle Preparation Method on the Particle Size Growth. In our previous study of the Suzuki reaction between phenylboronic acid and iodobenzene conducted using PVP–Pd nanoparticles,²² it was found that after the first cycle of the reaction, the center of distribution increased by $38 \pm 10\%$ and the width of distribution increased by $155 \pm 18\%$. This was attributed to Ostwald ripening²² of the nanoparticles, i.e., a result of dissolving the small sized nanoparticles to feed the growth of the larger ones that have lower surface tension. It also could have resulted from the presence of metal atoms in solution, which continued to deposit on the nanoparticle surface. Of course, if the mechanism of the particle growth involved the reduction of the metal ions on the surface of the nanoparticle, excess metal ions in solution could have led to the observed nanoparticle size during the catalytic reaction.

After the second cycle of the reaction, the centers of distribution actually decreased by $24 \pm 3\%$ and the widths of distributions decreased by 68% compared to the size during the first cycle. This decrease in size was attributed to the aggregation of larger Pd nanoparticles leading to its precipitating out of solution, leaving only the smaller nanoparticles in solution. The

percentage increase/decrease in the centers and widths of distributions after the first and second cycle are summarized in Table 2.

The stability of the PAMAM–OH generation 4 dendrimer-capped Pd nanoparticles after the first and second cycle of the Suzuki reaction was also investigated to gain a better understanding of the nanoparticle growth process. Table 1 summarizes the centers and widths of the distributions determined from Gaussian fits for various perturbations that were conducted. Parts a and b of Figure 1 show typical TEM image and Gaussian fits of the size distributions of PAMAM–OH generation 4 dendrimer-capped Pd nanoparticles before the Suzuki reaction. It can be seen that the nanoparticles are very small in size (1.3 ± 0.1 nm) and also reasonably monodispersed. These nanoparticles are smaller in size than the PVP–Pd nanoparticles²² (2.1 ± 0.1 nm) studied previously. Parts c and d of Figure 1 show typical TEM image and Gaussian fits of the dendrimer-capped Pd nanoparticles after the first cycle of the Suzuki reaction. Table 2 summarizes the percentage increase/decrease in the centers and widths of distributions after the first and second cycle. Both the centers and widths of the size distributions increase by 54% and 186%, respectively, after the first cycle of the reaction. This increase in size of the nanoparticles could be attributed to Ostwald ripening of the nanoparticles. Parts e and f of Figure 1 show representative TEM image and Gaussian fits of the nanoparticles after the second cycle of the Suzuki reaction. During the second cycle, the dendrimer–Pd nanoparticles continue to increase in size with a 35% increase in the center and a 14% increase in the width of the distribution compared to the first cycle. This suggests that when the dendrimer–Pd nanoparticles are used, the growth process continues during the second cycle of the Suzuki reaction. The mechanism of the growth of the palladium nanoparticles is discussed in the next section.

Mechanism of Growth of the Palladium Nanoparticles.

There are several possibilities that could result in the large growth of the dendrimer–Pd nanoparticles such as high metal or metal ion concentration in solution resulting from the synthetic procedure, a large nanoparticle distribution in the beginning, and better capping making the rate of conversion to full nanoparticles slow, thus leading to an increase in the metal

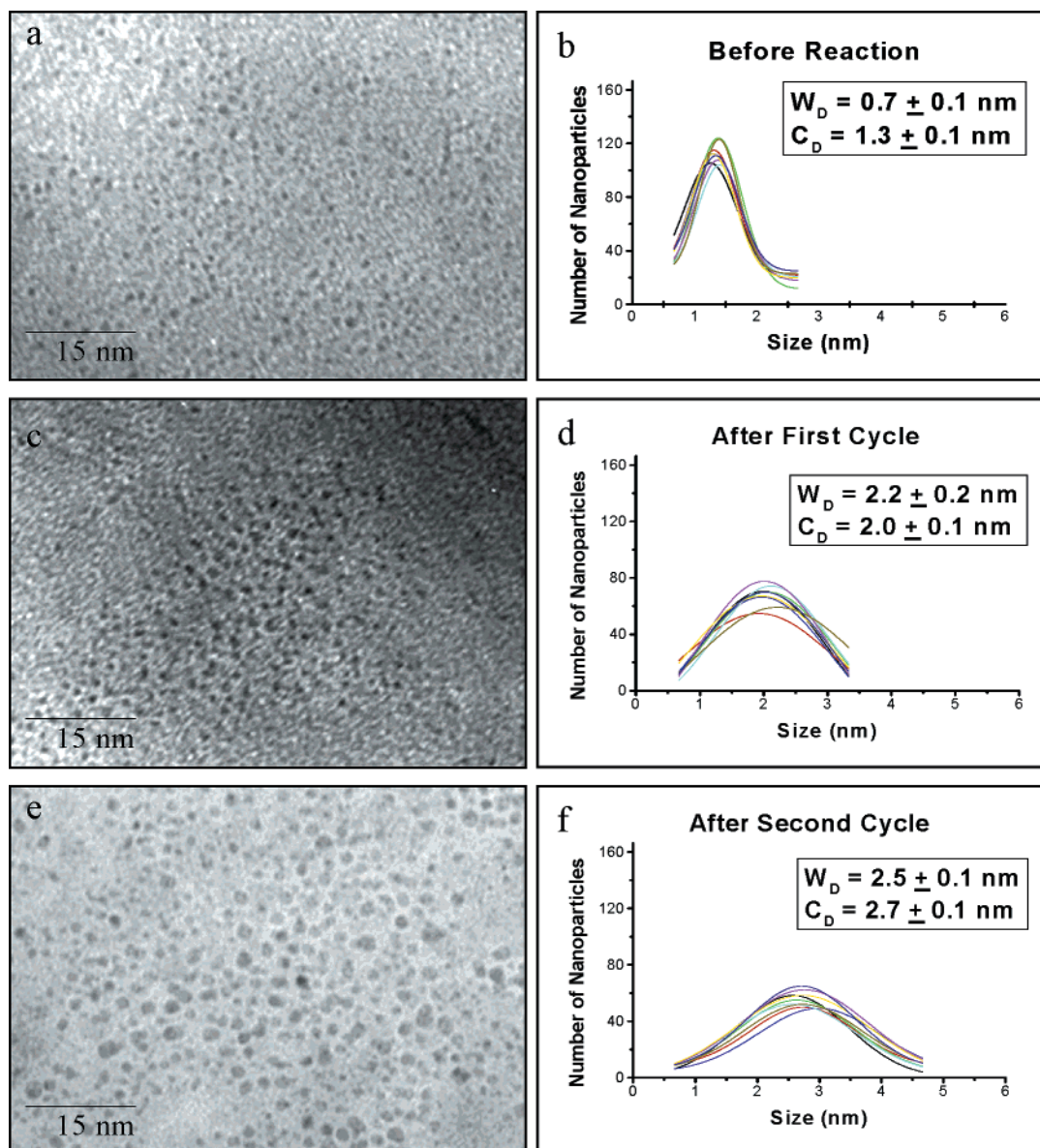


Figure 1. TEM images and Gaussian fits of size distributions of PAMAM-OH dendrimer-capped Pd nanoparticles before the Suzuki reaction (a, b), after the first cycle (c, d), and after the second cycle (e, f).

or metal ion concentration in the final solution. The large initial particle distribution could result in growth by the Ostwald ripening processes. The Ostwald ripening process is a mechanism for cluster growth in which there is detachment of atoms from the smaller clusters and attachment to the lower energy surfaces of the larger clusters. The smaller clusters shrink or disappear completely whereas the larger clusters grow in size and will eventually lead to larger nanoparticles with smaller width of distribution (more monodispersed).

It is worth noting that the PVP-Pd nanoparticles we studied previously²² were synthesized using the ethanol reduction method whereas the PAMAM-OH generation 4 dendrimer-capped Pd nanoparticles were synthesized using the sodium borohydride reduction method. The two types of nanoparticles were synthesized using two different reduction methods. Different methods of preparing nanoparticles vary in their degree of conversion of the metal ion into capped nanoparticles. PAMAM-OH generation 4 dendrimer-Pd nanoparticles are known to be very strong encapsulators of metal clusters.⁴⁰ Because the synthesis of the dendrimer-Pd nanoparticles occurs at room temperature, it is quite possible that the rate of

conversion to full nanoparticle is slow, thus leading to an increase in the metal or metal ion concentration in the final solution. This could also explain why the dendrimer-Pd nanoparticles are very small to begin with. During the Suzuki reaction, it is possible that the nanoparticles continue to grow in size because the rate of conversion to full nanoparticle is greater due to the high temperature and long reflux time period involved. This can also explain the continued growth of the nanoparticle size during the second cycle. The growth of the nanoparticles is expected to continue until the source of free metal is depleted. Because the widths of the size distributions of the dendrimer-Pd nanoparticles are broad during both the first and second cycle, as shown in Figure 1c-f, Table 1, and Table 2, the growth of the nanoparticles is not dominantly due to Ostwald ripening process but, instead, is largely due to the excess atoms or ions in solution during the catalytic reaction.

To test our hypothesis that the growth of the nanoparticles is due to the presence of unreduced ions, partly reduced ions, and metal atoms in solution after the synthesis of the nanoparticles, we conducted the reaction with dendrimer-Pd nanoparticles synthesized by reduction for 30 min and 3 h at room temper-

TABLE 3: Comparison of Center and Width of Size Distributions of Dendrimer–Pd Nanoparticles Synthesized with Various Reduction Times and Temperatures before the Reaction, after the First Cycle, and after the Second Cycle

| condition | before reaction (nm) | after first cycle (nm) | after second cycle (nm) |
|------------------------------------|--|--|--|
| reduced 30 min at room temperature | $C_D = 1.4 \pm 0.1$ $W_D = 0.7 \pm 0.1$ | $C_D = 2.1 \pm 0.1$ $W_D = 2.4 \pm 0.2$ | $C_D = 2.9 \pm 0.1$ $W_D = 2.8 \pm 0.4$ |
| reduced 1 h at room temperature | $C_D = 1.3 \pm 0.1$ $W_D = 0.7 \pm 0.1$ | $C_D = 2.0 \pm 0.1$ $W_D = 2.2 \pm 0.2$ | $C_D = 2.7 \pm 0.1$ $W_D = 2.5 \pm 0.1$ |
| reduced 3 h at room temperature | $C_D = 1.4 \pm 0.1$ $W_D = 0.7 \pm 0.1$ | $C_D = 2.0 \pm 0.2$ $W_D = 1.9 \pm 0.1$ | $C_D = 2.5 \pm 0.1$ $W_D = 2.2 \pm 0.2$ |
| reduced 1 h at 100 °C | $C_D = 1.5 \pm 0.1$ $W_D = 0.7 \pm 0.1$ | $C_D = 1.8 \pm 0.1$ $W_D = 1.7 \pm 0.2$ | $C_D = 2.1 \pm 0.1$ $W_D = 2.0 \pm 0.2$ |

ature. We also conducted the reaction with dendrimer–Pd nanoparticles synthesized by reduction for 1 h at 100 °C. The standard procedure reported in the literature^{41–43} for synthesizing dendrimer–Pd nanoparticles involves reduction for 1 h at room temperature, which is what we based all of our experiments on. The goal now is to see if the growth process is affected by the amount of reduction time or the reduction temperature at which the nanoparticles are initially synthesized. Table 3 summarizes the average size and widths of distributions of the dendrimer–Pd nanoparticles before the reaction, after the first cycle, and after the second cycle for the following synthetic conditions (reduction for 30 min at room temperature, reduction for 1 h at room temperature (standard procedure), reduction for 3 h at room temperature, and reduction for 1 h at 100 °C). Figure 2 a–h shows typical TEM images and Gaussian fits of the size distributions of the dendrimer–Pd nanoparticles after the second cycle for the four different synthetic conditions. The entry for 1 h at room temperature in Table 3 is repeated from Table 1 and the TEM image and Gaussian fits in Figure 2c,d is repeated from Figure 1e,f for comparison purposes. It can be seen that the general trend observed is that the growth of the dendrimer–Pd nanoparticles is the greatest using the nanoparticles reduced for only 30 min and the growth is the lowest when the nanoparticles are reduced for 1 h at 100 °C. This suggests that reduction at room temperature for a longer time period and reduction at 100 °C results in a more complete reduction of the precursor palladium salt. As a result, there are fewer free metal atoms and ions present in solution to contribute to the growth during the reaction. This trend supports our hypothesis that the growth process is dependent on the amount of free atoms or ions present after the synthetic process.

Effect of Capping Agent on Mechanism of Suzuki Reaction. For the PVP–Pd nanoparticles catalyzing the Suzuki reaction studied previously,²² it was determined that the Ostwald ripening process occurred when refluxing in the presence of iodobenzene, whereas refluxing in the presence of phenylboronic acid results in the inhibition of the nanoparticle size growth. It was proposed that phenylboronic acid binds to the nanoparticle surface and acts as a capping agent which protects the particles from increasing in size. The mechanism was proposed to involve the phenylboronic acid binding to the nanoparticle surface whereas reaction with iodobenzene occurs via collisional processes.

The stability of the PAMAM–OH generation 4 dendrimer-capped palladium nanoparticles in the presence of various chemicals involved in the Suzuki reaction (solvent, sodium acetate, phenylboronic acid, and iodobenzene) was investigated to find out if the mechanism of the reaction is affected by the capping agent that is used on the palladium nanoparticles. TEM images and Gaussian fits of the size distributions of the nanoparticles were obtained before each perturbation and the results are summarized in Table 1. To concisely summarize the results, the TEM images and Gaussian fits of the size distributions of the dendrimer–Pd nanoparticles after the different

perturbations are shown in Figure 3. Parts a and b of Figure 3 show a representative TEM image and Gaussian fits for the nanoparticles after refluxing in solvent alone, and Parts c and d of Figure 3 show a typical TEM image and Gaussian fits of the nanoparticles after refluxing in solvent + sodium acetate. In both cases, the growth of the nanoparticles is evident because the widths and centers of the size distributions of the nanoparticles increases. Parts e and f of Figure 3 show a representative TEM image and Gaussian fits of the nanoparticles after refluxing in solvent + sodium acetate + phenylboronic acid. It can be seen that the growth of the nanoparticles is inhibited because the nanoparticle size does not increase much. This was also observed with the PVP–Pd nanoparticles previously.²² The phenylboronic acid in its deprotonated form acts as a capping agent and binds to many of the free Pd sites on the nanoparticles and inhibits the growth process. Parts g and h of Figure 3 show representative TEM image and Gaussian fits of the nanoparticles after refluxing in solvent + sodium acetate + iodobenzene. Growth of the nanoparticles occurs in this case because iodobenzene probably does not bind to the nanoparticle surface.

On the basis of the results, it can be seen that the mechanism of phenylboronic acid binding to the nanoparticle surface and reacting with iodobenzene in solution also occurs when the PAMAM–OH generation 4 dendrimer-capped Pd nanoparticles are used to catalyze the Suzuki reaction. Because the mechanism observed is the same for both the PVP–Pd nanoparticles studied previously²² and for the dendrimer–Pd nanoparticles studied presently, it can be concluded that the mechanism of the reaction is insensitive to the capping agent used.

Effect of Nanoparticle Size during Second Cycle on Biphenyl Yield. For the PVP–Pd nanoparticles studied previously,²² the yield of biphenyl after the first and second cycle was determined using HPLC and it was observed that the catalytic activity of the nanoparticles is greatly diminished during the second cycle of the Suzuki reaction. The results obtained previously are reported in Table 4 as concentration of biphenyl and % yield of biphenyl. The % yield is obtained on the basis of the amount of biphenyl actually formed compared to the theoretical amount of biphenyl that can be formed. The theoretical yield of biphenyl is 1 mmol because iodobenzene is the limiting reagent and there is only 1 mmol iodobenzene present at the beginning of the reaction. The ratio of (biphenyl yield_{second})/(biphenyl yield_{first}) when the PVP–Pd nanoparticles are used is 0.38 ± 0.08 , as shown in Table 5. The diminished catalytic activity observed was attributed to two effects. The aggregation and precipitation of the larger nanoparticles out of solution could result in the smaller nanoparticles remaining in solution, and the biphenyl product itself could poison some of the active sites of the PVP–Pd nanoparticles. It is also worth mentioning that precipitation of the nanoparticles was observed in the bottom of the solution after catalysis.

The catalytic activity of the PAMAM–OH generation 4 dendrimer-capped Pd nanoparticles was also studied using

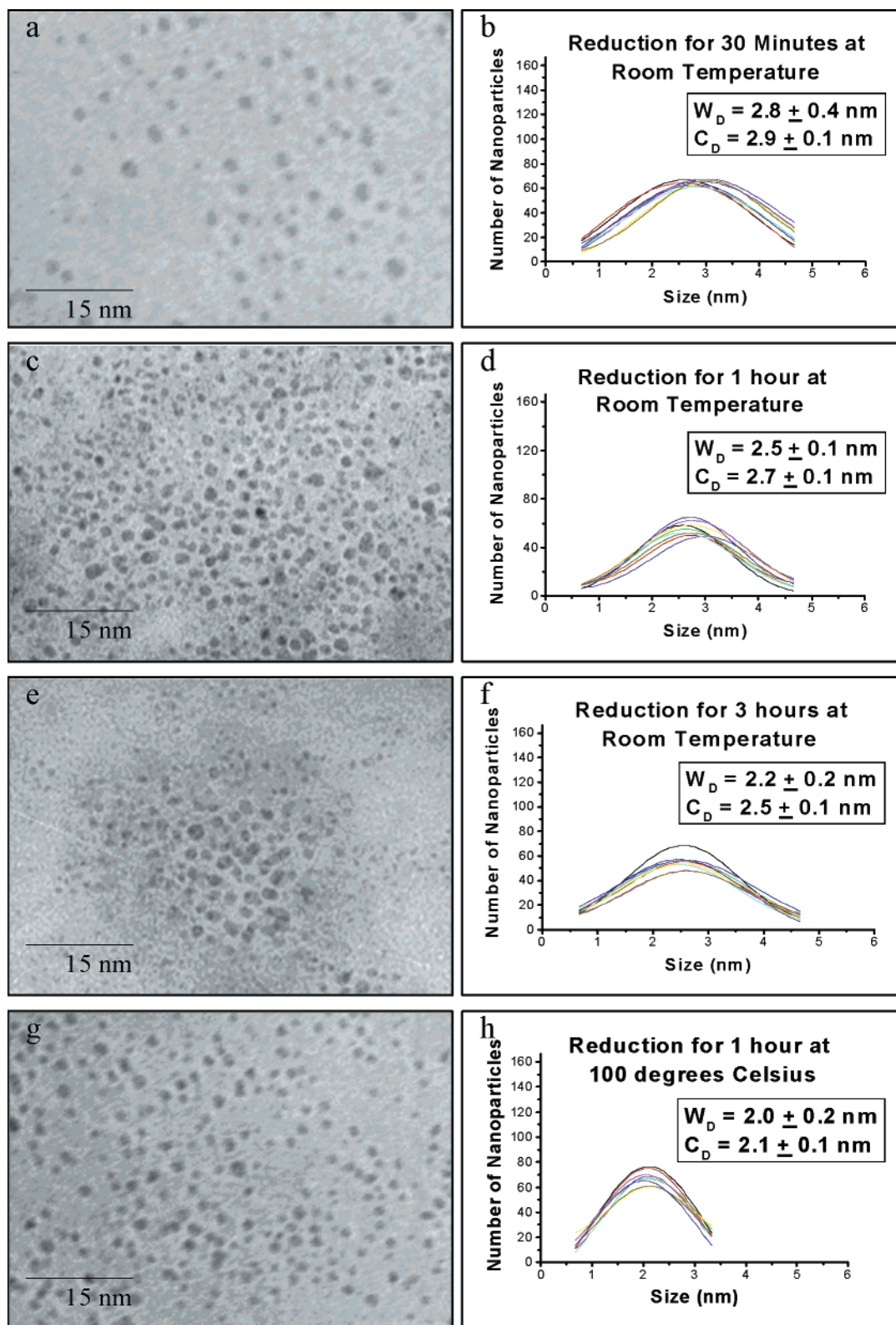


Figure 2. Typical TEM images and Gaussian fits of the size distributions after the second cycle of the Suzuki reaction for dendrimer-Pd nanoparticles synthesized in the following manners: reduction for 30 min at room temperature (a, b), reduction for 1 h at room temperature (c, d), reduction for 3 h at room temperature (e, f), and reduction for 1 h at 100 °C (g, h).

HPLC and compared to that of the PVP-Pd nanoparticles. The HPLC results on the concentration and % biphenyl yield obtained using the PAMAM-OH generation 4 dendrimer-capped Pd nanoparticles as the catalyst are summarized in Table 4. When the dendrimer-Pd nanoparticles are used as the catalyst, the catalytic activity is also diminished during the second cycle of the Suzuki reaction but not as much as observed

with the PVP-Pd nanoparticles. As shown in Table 5, the ratio of (biphenyl yield_{second})/(biphenyl yield_{first}) when the PAMAM-OH generation 4 dendrimer-capped Pd nanoparticles are used to catalyze the Suzuki reaction is 0.50 ± 0.09 . A possible reason the ratio of biphenyl yields is higher when the dendrimer-Pd nanoparticles are used is that the nanoparticles continue to grow during the second cycle, resulting in more active sites. Because

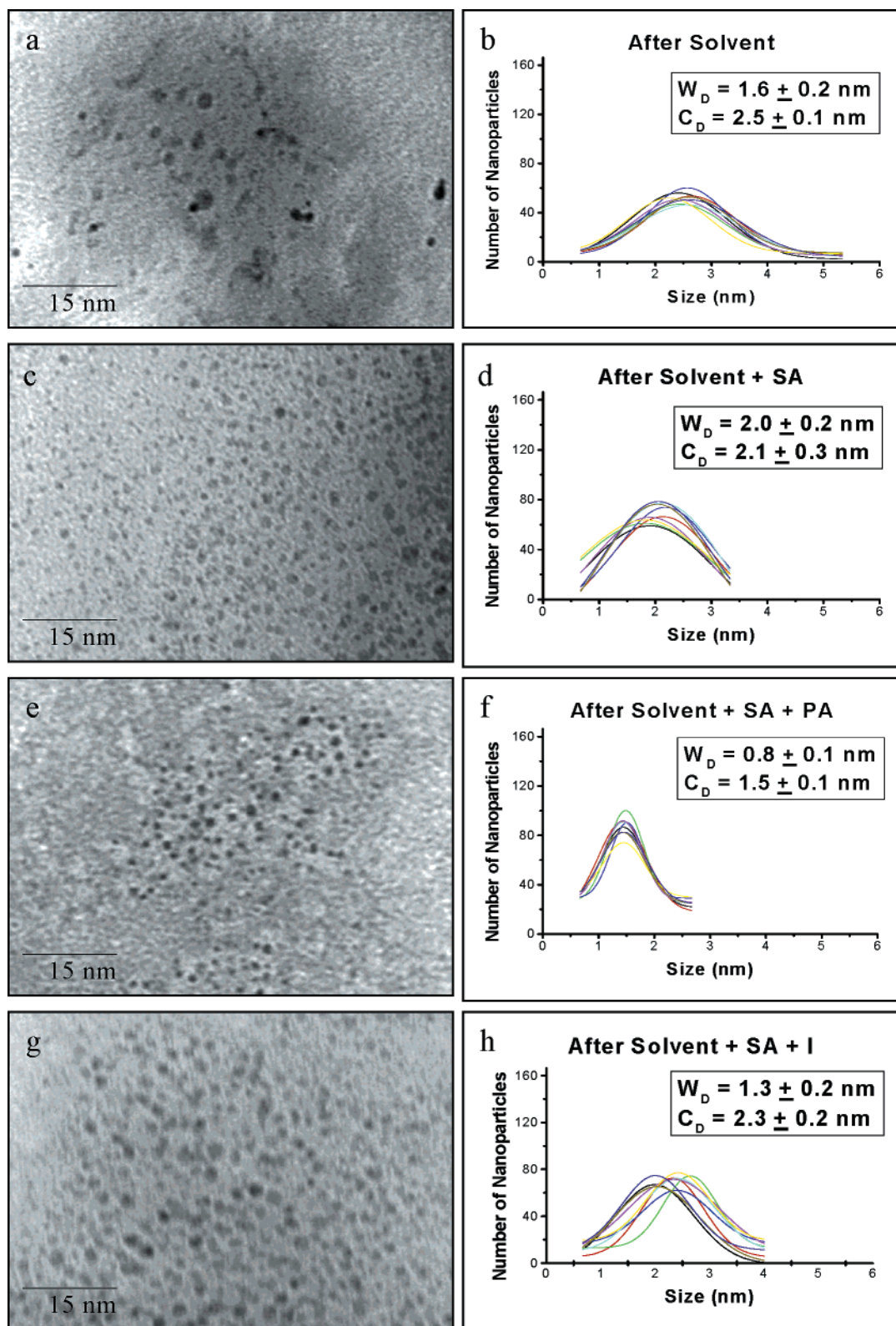


Figure 3. TEM images and Gaussian fits of the size distributions of PAMAM-OH generation 4 dendrimer-Pd nanoparticles after refluxing in solvent (a, b), after refluxing in solvent + SA (c, d), after refluxing in solvent + SA + PA (e, f), and after refluxing in solvent + SA + I (g, h).

the nanoparticles continue to increase in size, precipitation of the nanoparticles might not be taking place. This is also supported by the absence of the black metallic powder at the bottom of the reaction mixture after catalysis. This is expected to be the case as the dendrimer is a strong and stable capping agent. As a result, the diminished yield observed is probably due to poisoning of the active sites by the biphenyl product. The larger size of the dendrimer-Pd nanoparticles during the

second cycle could also contribute to the higher ratio of biphenyl yield with the dendrimer-Pd than with the PVP-Pd nanoparticles. The larger sized dendrimer-Pd nanoparticles have more active sites available for catalysis because these sites are less likely to be poisoned by biphenyl.

Effect of Excess Capping Agent. For the PVP-Pd nanoparticles studied previously,²² the effect of the addition of excess PVP to the reaction mixture was found to diminish the growth

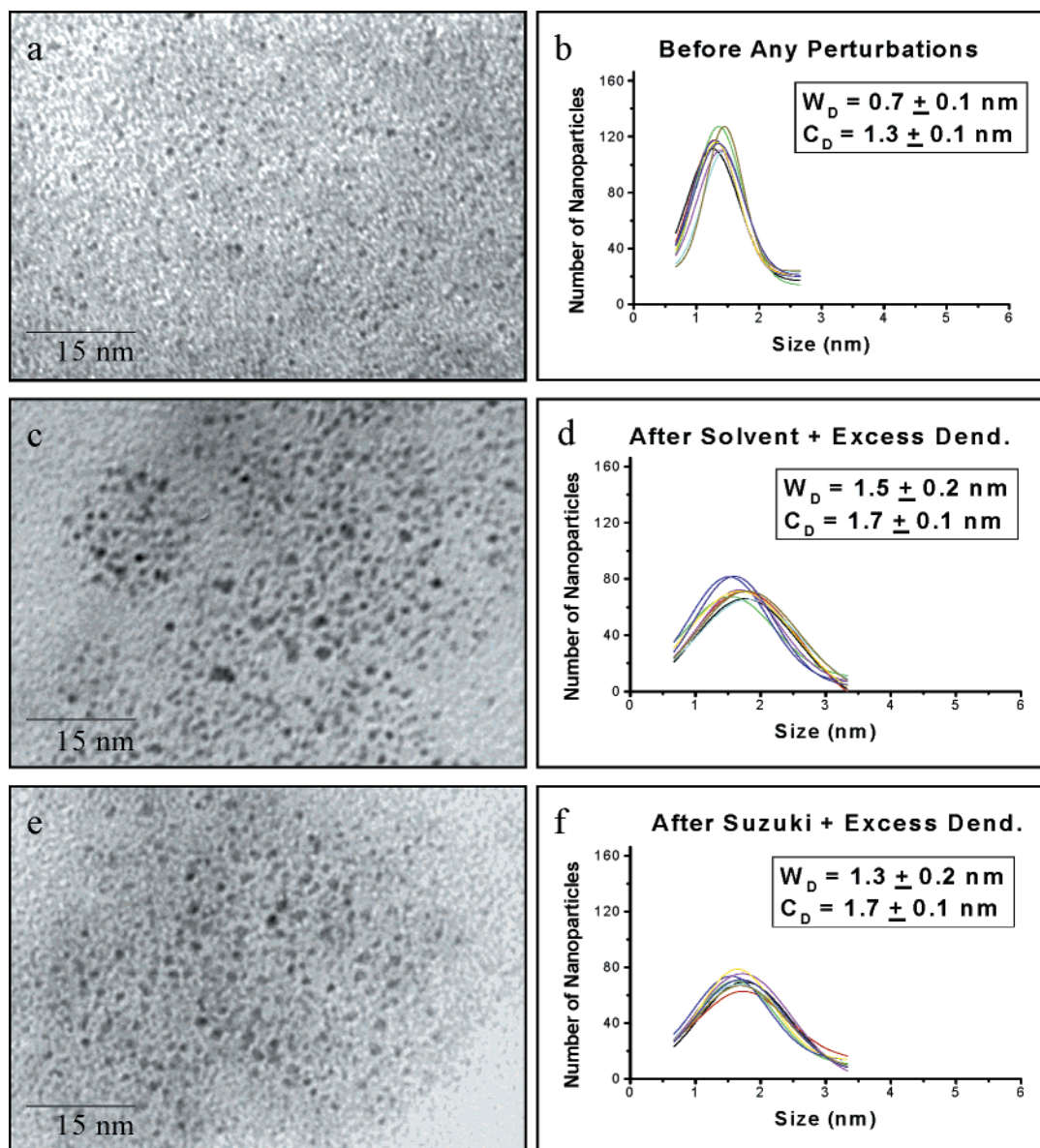


Figure 4. TEM images and Gaussian fits of the size distributions of PAMAM–OH generation 4 dendrimer–Pd nanoparticles before any perturbations (a, b), after refluxing in solvent + excess dendrimer (c, d), and after Suzuki reaction in the presence of excess dendrimer (e, f).

TABLE 4: Comparison of Concentration and Reaction Yield of Biphenyl in the Suzuki Reaction Catalyzed by the PVP–Pd Nanoparticles and Dendrimer–Pd Nanoparticles

| condition | concentration and % biphenyl yield using PVP–Pd nanoparticles ²² | concentration and % biphenyl yield using PAMAM–OH generation 4 dendrimer–Pd nanoparticles |
|--|---|---|
| first cycle | 3.00 ± 0.32 mM 39 ± 4% yield | 2.61 ± 0.21 mM 34 ± 3% yield |
| second cycle | 1.11 ± 0.20 mM 15 ± 3% yield | 1.31 ± 0.25 mM 17 ± 3% yield |
| after first cycle in presence of excess capping material | 2.28 ± 0.18 mM 30 ± 2% yield | 0.42 ± 0.05 mM 6 ± 1% yield |

processes as well as diminish the catalytic activity of the nanoparticles. The effect of adding excess dendrimer to the Suzuki reaction mixture was investigated with the PAMAM–OH generation 4 dendrimer–Pd nanoparticles and the HPLC results are summarized in Table 4. It can be seen that the addition of excess dendrimer severely diminishes the catalytic activity of the dendrimer–Pd nanoparticles. This is probably due to the strong encapsulating action of the generation 4 dendrimer on the nanoparticles. In addition, the dendrimer–Pd nanoparticles are smaller than the PVP–Pd nanoparticles studied previously and as a result, will have a smaller concentration of

TABLE 5: Ratios of Biphenyl Yields Obtained Using PVP–Pd Nanoparticles and PAMAM–OH Generation 4 Dendrimer–Pd Nanoparticles

| nanoparticle type | biphenyl yield ratio (2nd cycle/1st cycle) |
|--|--|
| PVP–Pd nanoparticles ²² | 0.38 ± 0.08 |
| PAMAM–OH generation 4 dendrimer–Pd nanoparticles | 0.50 ± 0.09 |

active sites on the surface that are available. The addition of excess dendrimer will thus result in a much lower number of active sites available for the catalysis to occur.

Figure 4 shows typical TEM images and Gaussian fits of the size distributions of the dendrimer–Pd nanoparticles before any perturbations (a, b), after refluxing in the presence of solvent and excess dendrimer (c, d), and after Suzuki reaction in the presence of excess dendrimer (e, f). It can be seen that the presence of excess dendrimer diminishes the growth of the nanoparticles when refluxed in solvent alone and when added to the Suzuki reaction mixture. This is also observed previously²² with the PVP–Pd nanoparticles.

Conclusions

The nanoparticle growth process observed in the reaction by refluxing in the solvent is governed by the amount of free metal present in solution after the preparation of the nanoparticles. Different methods of preparing nanoparticles result in varying amounts of free metal in solution. Because PAMAM–OH generation 4 dendrimer is a strong encapsulator, the rate of conversion to full nanoparticle is slow, resulting in the large concentration of metal in solution. It is shown that the mechanism of the Suzuki reaction in which phenylboronic acid binds to the nanoparticle surface and reacts with iodobenzene in solution is insensitive to the capping agent used. This is because the growth of the nanoparticles in the presence of iodobenzene and the inhibition of the growth in the presence of phenylboronic acid occurs for both the dendrimer–Pd nanoparticles and the PVP–Pd nanoparticles studied previously.²² The biphenyl ratio (second cycle/first cycle) is higher for the dendrimer–Pd nanoparticles than the PVP–Pd nanoparticles. This could be due to the dendrimer–Pd nanoparticles being larger during the second cycle and thus having more active sites and also due to the nanoparticles not precipitating out of solution yet. However, the biphenyl product itself probably still does poison some of the active sites on the nanoparticle surface. It is also found that the presence of excess dendrimer severely diminishes the catalytic activity of the nanoparticles and this is probably due to the strong encapsulating action of the generation 4 dendrimer to the nanoparticles resulting in a much lower number of sites available for catalysis. The presence of excess dendrimer is also found to diminish the growth process.

Acknowledgment. We thank the Electron Microscopy Center for the JEOL 100C TEM facility that we used for our TEM experiments. We also thank Dr. Gary Schuster's group for their HPLC, which we used to carry out the HPLC experiments. We also thank NSF (CHE-0240380) for funding.

References and Notes

- (1) Eppler, A.; Rupprechter, G.; Gucci, L.; Somorjai, G. A. *J. Phys. Chem. B* **1997**, *101* (48), 9973.
- (2) Toshima, N.; Yonezawa, T. *New J. Chem.* **1998**, *22* (11), 1179.
- (3) Schmid, G. *Met. Cluster Chem.* **1999**, *3*, 1325.
- (4) Puddephatt, R. J. *Met. Cluster Chem.* **1999**, *2*, 605.
- (5) Henry, C. R. *Appl. Surf. Sci.* **2000**, *164*, 252.
- (6) St. Clair, T. P.; Goodman, D. W. *Top. Catal.* **2000**, *13* (1, 2), 5.
- (7) Kralik, M.; Corain, B.; Zecca, M. *Chem. Pap.* **2000**, *54* (4), 254.
- (8) Chusuei, C. C.; Lai, X.; Luo, K.; Goodman, D. W. *Top. Catal.* **2001**, *14* (1–4), 71.
- (9) Bowker, M.; Bennett, R. A.; Dickinson, A.; James, D.; Smith, R. D.; Stone, P. *Stud. Surf. Sci. Catal.* **2001**, *133*, 3.
- (10) Kralik, M.; Biffis, A. *J. Mol. Catal. A: Chem.* **2001**, *177* (1), 113.
- (11) Thomas, J. M.; Raja, R. *Chem. Rec.* **2001**, *1* (6), 448.
- (12) Mohr, C.; Claus, P. *Sci. Prog.* **2001**, *84* (4), 311.
- (13) Thomas, J. M.; Johnson, B. F. G.; Raja, R.; Sankar, G.; Midgley, P. A. *Acc. Chem. Res.* **2003**, *36* (1), 20.
- (14) Bradley, J. S. *Cluster Colloids* **1994**, 459.
- (15) Duff, D. G.; Baiker, A. *Stud. Surf. Sci. Catal.* **1995**, *91*, 505.
- (16) Toshima, N. *NATO ASI Ser., Ser. 3* **1996**, *12*, 371.
- (17) Boenermann, H.; Braun, G.; Brijoux, G. B.; Brinkman, R.; Tilling, A. S.; Schulze, S. K.; Siepen, K. *J. Organomet. Chem.* **1996**, *520* (1–2), 143.
- (18) Fugami, K. *Organomet. News* **2000**, *1*, 25.
- (19) Mayer, A. B. R. *Polym. Adv. Technol.* **2001**, *12* (1–2), 96.
- (20) Bonnemant, H.; Richards, R. *Syn. Methods Organomet. Inorg. Chem.* **2002**, *10*, 209.
- (21) Moiseev, I. I.; Vargaftik, M. N. *Russ. J. Chem.* **2002**, *72* (4), 512.
- (22) Narayanan, R.; El-Sayed, M. A. *J. Am. Chem. Soc.*, **2003**, *125* (27), 8340.
- (23) Collier, P. J.; Iggo, J. A.; Whyman, R. *J. Mol. Catal. A: Chem.* **1999**, *146* (1–2), 149.
- (24) Sculz, J.; Roucoux, A.; Patin, H. *Chem. Eur. J.* **2000**, *6* (4), 618.
- (25) Wang, Q.; Liu, H.; Han, M.; Li, X.; Jiang, D. *J. Mol. Catal. A: Chem.* **1997**, *118* (2), 145.
- (26) Kim, S.; Son, S. U.; Lee, S. S.; Hyeon, T.; Chung, Y. K. *Chem. Commun.* **2001**, 2212.
- (27) Larpent, C.; Menn, B. F.; Patin, H. *J. Mol. Catal.* **1991**, *65*, L35.
- (28) Sidorov, S. N.; Volkov, I. V.; Davankov, V. A.; Tsyurupa, M. P.; Valetsky, P. M.; Bronstein, L. M.; Karlinsey, R.; Zwanziger, J. W.; Matveeva, V. G.; Sulman, E. M.; Lakina, N. V.; Wilder, E. A.; Spontak, R. J. *J. Am. Chem. Soc.* **2001**, *123* (43), 10502.
- (29) Chechik, V.; Crooks, R. M. *J. Am. Chem. Soc.* **2000**, *122*, 1243.
- (30) Yeung, L. K.; Crooks, R. M. *Nano Lett.* **2001**, *1* (1), 14.
- (31) Dupont, J.; Fonseca, G. S.; Umpierre, A. P.; Fichtner, P. F. P.; Teixeira, S. R. *J. Am. Chem. Soc.* **2002**, *124*, 4228.
- (32) Hirai, H.; Chawanya, H.; Toshima, N. *Nip. Kag. Kai.* **1984**, *6*, 1027.
- (33) Roucoux, A.; Sculz, J.; Patin, H. *Chem. Rev.* **2002**, *102* (10), 3757.
- (34) Zhao, M.; Sun, L.; Crooks, R. M. *J. Am. Chem. Soc.* **1998**, *120*, 4877.
- (35) Zhao, M.; Crooks, R. M. *Angew. Chem., Int. Ed. Engl.* **1999**, *38* (3), 364.
- (36) Chechik, V.; Zhao, M.; Crooks, R. M. *J. Am. Chem. Soc.* **1999**, *121*, 4910.
- (37) Chechik, V.; Crooks, R. M. *J. Am. Chem. Soc.* **2000**, *122*, 1243.
- (38) Rahim, E. H.; Kamounah, F. S.; Frederiksen, J.; Christensen, J. B. *Nano Lett.* **2001**, *1* (9), 499.
- (39) Zhao, M.; Crooks, R. M. *Adv. Mater.* **1999**, *11* (3), 217.
- (40) Kunio, E.; Keiko, M.; Tomokazu, Y. *J. Colloid Interface Sci.* **2002**, *254* (2), 402.
- (41) Li, Y.; El-Sayed, M. A. *J. Phys. Chem. B* **2001**, *105*, 8938.
- (42) Li, Y.; Hong, X. M.; Collard, D. M.; El-Sayed, M. A. *Org. Lett.* **2000**, *2* (15), 2385.
- (43) Li, Y.; Boone, E.; El-Sayed, M. A. *Langmuir* **2002**, *18*, 4921.